

Assessment of cartilage-dedicated sequences at ultra-high-field MRI: comparison of imaging performance and diagnostic confidence between 3.0 and 7.0 T with respect to osteoarthritis-induced changes at the knee joint

Robert Stahl · Roland Krug · Douglas A. C. Kelley ·
Jin Zuo · C. Benjamin Ma · Sharmila Majumdar ·
Thomas M. Link

Received: 21 December 2008 / Revised: 24 February 2009 / Accepted: 25 February 2009 / Published online: 18 March 2009
© The Author(s) 2009. This article is published with open access at Springerlink.com

Abstract

Objective The objectives of the study were to optimize three cartilage-dedicated sequences for in vivo knee imaging at 7.0 T ultra-high-field (UHF) magnetic resonance imaging (MRI) and to compare imaging performance and diagnostic confidence concerning osteoarthritis (OA)-induced changes at 7.0 and 3.0 T MRI.

Materials and methods Optimized MRI sequences for cartilage imaging at 3.0 T were tailored for 7.0 T: an intermediate-weighted fast spin-echo (IM-w FSE), a fast imaging employing steady-state acquisition (FIESTA) and a T1-weighted 3D high-spatial-resolution volumetric fat-suppressed spoiled gradient-echo (SPGR) sequence. Three

healthy subjects and seven patients with mild OA were examined. Signal-to-noise ratio (SNR), contrast-to-noise ratio (CNR), diagnostic confidence in assessing cartilage abnormalities, and image quality were determined. Abnormalities were assessed with the whole organ magnetic resonance imaging score (WORMS). Focal cartilage lesions and bone marrow edema pattern (BMEP) were also quantified.

Results At 7.0 T, SNR was increased ($p < 0.05$) for all sequences. For the IM-w FSE sequence, limitations with the specific absorption rate (SAR) required modifications of the scan parameters yielding an incomplete coverage of the knee joint, extensive artifacts, and a less effective fat saturation. CNR and image quality were increased ($p < 0.05$) for SPGR and FIESTA and decreased for IM-w FSE. Diagnostic confidence for cartilage lesions was highest ($p < 0.05$) for FIESTA at 7.0 T. Evaluation of BMEP was decreased ($p < 0.05$) at 7.0 T due to limited performance of IM-w FSE.

Conclusion Gradient echo-based pulse sequences like SPGR and FIESTA are well suited for imaging at UHF which may improve early detection of cartilage lesions. However, UHF IM-w FSE sequences are less feasible for clinical use.

R. Stahl · R. Krug · J. Zuo · S. Majumdar · T. M. Link
Musculoskeletal and Quantitative Imaging Group,
Department of Radiology, University of California,
San Francisco, 185 Berry Street, Suite 350,
San Francisco, CA 94107-0946, U.S.A.

R. Stahl (✉)
Department of Clinical Radiology,
University Hospitals—Campus Grosshadern,
Ludwig Maximilians University of Munich,
Marchioninistrasse 15,
Munich 81377, Germany
e-mail: Robert.Stahl@radiology.ucsf.edu

D. A. C. Kelley
General Electrics (GE) Healthcare Technologies,
1700 4th Street, Suite 203,
San Francisco, CA 94158, U.S.A.

C. B. Ma
Department of Orthopedic Surgery, University of California,
San Francisco, 500 Parnassus Ave MU-320W,
San Francisco, CA 94143-0728, U.S.A.

Keywords Knee · Magnetic resonance imaging ·
Ultra-high-field technology · Cartilage imaging ·
Cartilage lesions

Introduction

High-field (HF) magnetic resonance (MR) systems operating at a field strength (B_0) of 3.0 T have shown promise for musculoskeletal imaging [1–9] and are increasingly utilized in clinical practice [6]. The approximately twofold increase

in signal to noise ratio (SNR) translates into better visualization of anatomical and pathological structures. This has been shown to be particularly beneficial for imaging cartilage and ligaments [1–5, 7, 8].

Recently, ultra-high-field (UHF) whole body scanners with a B_0 of 7.0 T have become available in a few research centers [10, 11]. Consequently, there is an interest in exploring the potential of this technique for musculoskeletal imaging. The signal-to-noise ratio (SNR) is expected to be almost linearly related to B_0 . At higher field strengths, the increase of SNR could be used to improve spatial or temporal resolution. Drawbacks of higher field strength are an increase in susceptibility artifacts and in chemical shift artifacts [6, 11]. For the latter, the receiver bandwidth has to be increased which causes significant signal loss. Additionally, at higher Larmor frequencies, the dielectric properties of the tissue generally act to enhance the radiofrequency (RF) magnetic field within tissue. However, conductivity also generally increases with frequency, albeit weakly, which tends to limit RF field penetration as well as suppressing a true dielectric resonance within the tissue. Thus, RF power increases with higher B_0 and with standard sequences limits of the specific absorption rate (SAR) may be exceeded. The homogeneity of the RF magnetic field (B_1) decreases in large organs. Inhomogeneous power absorption can lead to the formation of hot-spots. Alterations in field strength also change tissue relaxation characteristics necessitating an adjustment of the appropriate repetition time (TR) and echo time (TE) to obtain optimal SNR and contrast.

To the best of our knowledge, only one study [12] has investigated a set of MRI sequences (short T1 inversion recovery (STIR), proton-density, and T2 weighted turbo spin echo (PD-T2 TSE), multi echo data image combination (MEDIC), and dual-echo steady-state (DESS)) for 7.0 T imaging of the knee and compared those to standard sequences used on a 1.5-T scanner. The diagnostic value of a specific subset of cartilage-dedicated sequences for OA-induced changes has not been assessed using UHF techniques and compared to HF techniques.

Thus, the goals of our study were (1) to adapt a set of cartilage-dedicated sequences, which have been previously optimized for 3.0 T [3] (fat-saturated intermediate-weighted fast spin-echo (IM-w FSE), T1-weighted 3D high-spatial-resolution volumetric fat-suppressed spoiled gradient-echo (SPGR), and fast imaging employing steady-state acquisition with constructive interference in steady state (3D FIESTA-C)) for imaging at 7.0 T and demonstrate the feasibility of cartilage imaging using UHF, (2) to assess the imaging performance in terms of SNR, contrast-to-noise ratio (CNR), diagnostic confidence in assessing the presence and absence of abnormalities, and global image quality, and (3) to compare pathologic findings of the knee between 3.0 and

7.0 T in a cohort of ten subjects by using the Whole-Organ Magnetic Resonance Imaging Score (WORMS, [13]) as well as by quantification of the extent of cartilage abnormalities and bone marrow edema pattern (BMEP).

Material and methods

Subjects and clinical assessment

Seven patients with mild osteoarthritis (OA) (43.57 ± 11.97 years, four male, three female) were recruited for the study. They showed clinical symptoms and mild radiographic signs of knee OA: four of them had grade 1 OA, the remaining presented with grade 2 OA based on the Kellgren–Lawrence (KL) score [14]. In addition, three male healthy controls (36.00 ± 4.24 years) without clinical evidence of knee OA were examined. Exclusion criteria for all subjects were any contraindications for MRI. Written informed consent was obtained from all subjects after the nature of the examinations had been fully explained. All exams were performed in accordance with the rules from the local Human Research Committee.

Imaging

MRI imaging of the same knee joint of each subject was performed on a 3.0- and 7.0-Tesla system (Signa, GE Medical Systems, Waukesha, WI, USA) within 2 weeks. At both field strengths, a dedicated quadrature knee coil was employed (Clinical MR Solutions, Brookfield, WI, USA at 3.0 T and Nova Medical, Wilmington, MA, USA at 7.0 T) Transmit gain and shimming were manually adjusted.

The morphology of cartilage, menisci, ligaments and other knee structures was assessed on three sagittal cartilage dedicated pulse sequences: (1) a fat-saturated intermediate-weighted fast spin-echo sequence (IM-w FSE), (2) a T1-weighted 3D high-spatial-resolution volumetric fat-suppressed spoiled gradient-echo (SPGR) sequence, and (3) a 3D FIESTA-C (fast imaging employing steady-state acquisition with constructive interference in steady state, CISS) sequence. The CISS method [15–18] is preferably applied at higher fields in order to reduce susceptibility artifacts due to magnetic field inhomogeneities.

The parameters used for the sequences are shown in Table 1 and are results of a preceding optimization study: the optimal parameters at 3.0 T to achieve the best image quality within a clinically acceptable time frame has been described [3]. Great care was taken to use a similar setting at 7.0 T and keep the parameters constant to allow comparison between the two field strengths. However, since T1 relaxation time increases and T2 relaxation time decreases at higher field strength [10, 11, 17], it was necessary to repeat the optimization procedure at 7.0 T.

Table 1 Synopsis of the parameters used for all cartilage dedicated sequences

Field strength	IM-w		SPGR		FIESTA-C	
	3.0T	7.0T	3.0T	7.0T	3.0T	7.0T
Type	2D	2D	3D	3D	3D	3D
TR [ms]	4,300	8,000	16.72	16.96	8.50	7.23
TE [ms]	51	45	8.42	5.54	4.12	3.51
NEX	1	2	0.75	0.75	1	1
ETL	9	8	1	1	1	1
Slice thickness [mm]	2	2	1	1	1	1
BW [Hz/pixel]	122	122	122	122	163	163
Gap [mm]	0.5	0.5	0	0	0	0
Slices [#]	45	30	92	98	90	100
FOV [cm]	14	16	16	16	13	13
Flip angle [degree]	90	90	12	12	15	15
In-plane resolution [mm]	0.293×0.293	0.313×0.313	0.313×0.313	0.313×0.313	0.254×0.254	0.254×0.254
Acquisition matrix	512×256	512×256	512×512	512×512	320×320	320×320
k-space sampling [%]	100	100	75	75	100	100
Reconstruction matrix	512×512	512×512	512×512	512×512	512×512	512×512
TA [min:s]	12:42	N/A	07:37	10:01	08:42	07:40

TR repetition time, TE echo time, NEX number of excitations, FOV field of view, TA acquisition time, N/A not available due to multiple interruptions to stay within the SAR limits

Using these relaxation times, Krug et al. [17] have previously optimized pulse sequences for cartilage, based on numerical simulations of the Bloch equations. The flip angle and TE of FIESTA and SPGR were optimized to yield maximum contrast between cartilage, joint fluid, and menisci. Since conventional fat suppression methods would disturb the steady state of FIESTA, we adapted a different method by changing TE. A prolonged TE due to full Fourier acquisition resulted in less bone marrow signal due to more off-resonance effects at bone and bone marrow transitions and thus better contrast [17]. Most of these optimizations can be made by simulations and directly translated to the scanner. However, at 7.0 T, further restrictions have to be considered and are mainly related to the increased power deposition, which affects the safety of the subject. Thus, additional optimizations had to be made for the FSE sequence experimentally taking *in vivo* conditions (mainly imaging time and the specific absorption rate SAR) into account. This was performed in the three healthy subjects without clinical findings of knee pathology and was conducted similar to the procedure described in [7, 19]. Optimizing the IM-w sequence proved to be challenging: FSE sequences are characterized by a series of rapidly applied 180° rephasing pulses which at higher field strength require the application of higher radiofrequency energy. Since the SAR has to be kept within the Food and Drug Administration (FDA) limits of 3.2 W/kg, the scanner automatically interrupted the data acquisition during this sequence and

paused frequently for several minutes. In order to cover as much of the knee as possible with a minimal number of interruptions, TR was extended, and echo train length (ETL) was reduced. However, even with this compromise only 30 slices could be obtained.

Image analysis

All images were reviewed on PACS workstations (Agfa, Ridgefield Park, NJ, USA). Two radiologists with 19 and 5 years experience in musculoskeletal imaging assessed pathologic findings of the knee joint as well as diagnostic confidence within each sequence and image quality independently. They were blinded with regard to the field strength. In case of divergent results, an agreement was achieved with a consensus reading.

SNR and CNR calculations

SNR and CNR were measured for each sequence for both field strengths by the two radiologists (TML and RS) in consensus. SNR for cartilage was measured as the ratio of the mean signal intensity and the SD of the background noise, measured in a region of almost no signal. For consistency, ROIs were placed at identical positions on each image. Values were obtained for cartilage at the lateral patella, at the lateral femoral condyle, and at the lateral tibia. The average of these three results was calculated. The

CNR between cartilage and bone was defined as follows: $(\text{mean signal intensity}_{\text{cartilage}} - \text{mean signal intensity}_{\text{bone}}) / \text{SD}_{\text{background noise}}$. The ROI for bone was placed in the bone marrow of the femoral condyles. For the calculation of the signal intensity of cartilage, the same anatomical regions were used as described above. Again, the average of these results was calculated.

Scoring of pathologic findings

Pathologic findings at the knee joint were analyzed using a modified WORMS score [13]. The 15 previously described compartments were merged to a total of seven compartments: the medial and lateral tibia, trochlea, medial and lateral femur, as well as medial and lateral patella. Flattening or depression of the articular surfaces was not evaluated. Cartilage signal and morphology, marginal osteophytes, medial and lateral meniscal integrity, synovitis/effusion, intraarticular loose bodies and periarticular cysts/bursitis, anterior and posterior cruciate ligament integrity, as well as medial and lateral collateral ligament integrity were scored as suggested by the original WORMS score. To characterize the extent of the regional involvement of bone marrow edema and subchondral cysts, the original partitions of the femoral condyles and tibial plateaus in anterior, central, and posterior regions were used. Any other pathologies not included in a WORMS category score were also documented.

To better quantify small cartilage lesions, the volume of cartilage inhomogeneity (WORMS score=1) and the volume of cartilage defects (WORMS score \geq 2) were calculated on the sagittal IM-w FSE images as previously described [3]. Briefly, in lesions with a WORMS score of 1, the size of the signal inhomogeneity was quantified by multiplying its largest diameter with the number of slices that visualized it (slice thickness in mm including section gap). The volume of focal cartilage defects (WORMS score \geq 2) was approximated by the following equation:

$$\begin{aligned} \text{Lesion volume} = & \text{largest diameter [mm]} \times \text{number of sections} \\ & \times \text{section thickness including gap [mm]} \times \text{depth} \\ & \times \text{shape factor} \end{aligned}$$

The depth of the lesion was determined by dividing the surrounding normal cartilage into three layers with equal thickness. If the maximum lesion depth did not exceed the thickness of the superficial layer it was assigned as 1/3. It became 2/3 or 3/3 if the maximal lesion depth comprised also the medium or the lowest layer, respectively.

The shape factor was 1 if more than 50% of the lesion had the largest depth (assessed in the section with the largest diameter), otherwise a shape factor of 0.5 was assigned. Extent of bone marrow edema pattern was assessed on the IM-w FSE images by multiplying the two largest diameters with the number of sections, where it was visualized (slice thickness including gap).

Reproducibility of the quantitative measures

The precision of the two radiologists in the quantification of the extents of cartilage signal inhomogeneities, cartilage defects, and bone marrow edema at both field strengths was expressed by calculating the percentage coefficient of variation (CV%) as previously outlined by Gluer et al [20].

Assessment of level of confidence in diagnosing knee pathology

Both radiologists were asked to rate the confidence level for each compartment regarding the presence or absence of cartilage abnormalities and BMEP for each sequence at both field strengths. The following grading system was used: 1 “definitely no lesion,” 2 “most likely no lesion,” 3 “questionable lesion,” 4 “most likely a lesion,” 5 “definitely a lesion.” In addition, they used this grading system to rate the confidence level for meniscal lesions and integrity of the cruciate ligaments.

Based on the above definitions, a “diagnostic confidence score” for cartilage abnormalities and BMEP was calculated. The objective for this score was to provide a global measure of the diagnostic confidence for each sequence at each field strength in order to permit comparisons. It considers the certainty of the diagnosis by assigning different weight factors to the confidence levels. The score was calculated for each compartment including all studied subjects:

$$\begin{aligned} \text{Diagnostic confidence score} = & \text{Number of subjects with "definitely no lesion" in this compartment} \\ & - 0.5 \times \text{Number of subjects with "most likely no lesion" in this compartment} \\ & - \text{Number of subjects with "questionable a lesion" in this compartment} \\ & - 0.5 \times \text{Number of subjects with "most likely a lesion" in this compartment} \\ & + \text{Number of subjects with "definitely a lesion" in this compartment} \end{aligned}$$

The more subjects with a high diagnostic certainty are found (“definitely no lesion” and “definitely a

lesion”) the higher the score for the specific sequence in the examined compartment will be. This value is

reduced by one count for each subject with a dubious diagnostic certainty (“questionable lesion”) in this compartment. It is also reduced but to a smaller amount (by 0.5 count) when the diagnosis was made with a high probability but not without doubt (subjects with “most likely a lesion” and “most likely no lesion”). In summary, the higher the score, the higher the global diagnostic confidence of the sequence.

Image quality

Overall image quality of the cartilage-dedicated sequences was graded according to a four-level scale. For this grading, sharpness of edges, amount of blurring and other artifacts, contrast between fluid and cartilage, contrast between fluid and soft tissue, and amount of noise were analyzed subjectively by each of the two radiologists independently. In case of divergent results, a consensus was found in a second session. Images graded as 1 had poor quality (limited diagnostic information, severe artifacts), while images graded as 4 had excellent image quality (e.g., good diagnostic quality, minor or no artifacts).

Statistical analysis

Data were initially assessed for normality with the Kolmogorov–Smirnov test. *T* tests for paired samples were used to compare the SNR and CNR calculations as well as the overall image quality scores for the individual sequences and field strengths. *T* tests for paired samples were also used to compare the size of cartilage abnormalities and BMEP between the two field strengths.

Differences in the frequency of observed cartilage abnormalities and BMEP between the two field strengths were evaluated with the Chi² test. Differences in the distribution of the WORMS (sub-)scores and the sequence confidence ratings between 3.0 and 7.0 T were assessed with the Wilcoxon signed-rank test. Results were adjusted with Bonferroni correction for multiple comparisons.

All evaluations were performed using the SPSS statistical package (Version 12, SPSS, Chicago, IL, USA). A level of significance of $p < 0.05$ was used throughout the study.

Results

All subjects completed the examinations in both scanners. The examination time for the IM-w sequence at 7.0 Tesla varied interindividually due to SAR restrictions between 21 and 33 min. Three subjects reported sensations of warming of the studied knee joint and of dizziness after being removed from the 7.0-T scanner.

SNR and CNR calculations

Results of SNR and CNR calculations are shown in Table 2. At 3.0 T, SNR was comparable between the IM-w and the FIESTA-C sequence. SNR for both sequences were statistically higher in comparison to the SPGR sequence ($p < 0.05$). At 7.0 T, the SNR of all sequences was increased when compared to 3.0 T (Fig. 1). However, this increase was significant ($p < 0.05$) only for the SPGR and FIESTA-C sequence. CNR at 3.0 T was significantly higher ($p < 0.05$) for the IM-w sequence than for the SPGR and FIESTA-C sequence. At 7.0 T, it increased significantly ($p < 0.05$) for the FIESTA-C sequence. CNR at 7.0 T was also elevated for the SPGR sequence; however, this increase was not significant. Regarding the IM-w sequence, CNR was considerably but not significantly reduced at 7.0 T in comparison to 3.0 T.

Focal knee pathology

Seventy compartments were analyzed. Eight focal cartilage inhomogeneities and 14 focal cartilage lesions as well as five areas of BMEP were observed. The whole knee WORMS score [median value (25th percentile, 75th percentile)] was 6 (2, 7.25) at 3.0 T and 7 (4, 8.75) at 7.0 T which was not significantly different ($p > 0.05$). In three out of ten subjects, findings were identical at both

Table 2 SNR and CNR (mean±SD) by field strength

Sequence	SNR		p-value	Factor SNR ^a	CNR		p-value	Factor CNR ^a
	3.0T	7.0T			3.0T	7.0T		
IM-w	20.9±4.4	29.1±16.4	0.296	1.4	17.5±4.4	3.7±20.6	0.217	0.4
SPGR	14.6±4.1	23.3±3.4	0.013	1.7	12.2±3.9	17.8±3.7	0.097	1.7
FIESTA-C	19.9±5.3	46.6±11.6	0.003	2.5	6.1±3.3	22.0±9.6	0.010	4.4

P-values in bold indicate significant differences on the 5% level of significance

^aData were calculated by dividing CNR at 7.0 T by CNR at 3.0 T.

field strengths. In six subjects, the cartilage in a total of 14 compartments was graded differently at the two field strengths: in nine compartments (64.3%), higher cartilage scores were found at 7.0 T compared to 3.0 T [cumulative WORMS cartilage score of these subjects: 8 (4.5; 12) at 7.0 T; 6 (3, 10.75) at 3.0 T]. Five lesions were localized at the femoral condyles and two at the patella, one each at the

medial tibia and the trochlea. Four of them were not visualized at 3.0 T and showed a cartilage defect at 7.0 T (Fig. 2).

Five (35.7%) lesions had higher cartilage scores at 3.0 T compared to 7.0 T [cumulative WORMS cartilage score of these subjects: 5 (1.75; 12.375) at 7.0 T; 6 (2.5, 12.5) at 3.0 T]. Three were located at the patella, one at the medial

Fig. 1 Representative sections of the lateral knee compartment in a 57-year old male with mild OA at 3.0 T (*left column*) and 7.0 T (*right column*). IM-w images (*upper row*): At 7.0 T, extensive chemical shift artifacts at the bone-cartilage interface (*dashed arrows*) and pulsation artifacts in the posterior parts of the bones (*solid arrows*) were observed. SNR for cartilage was higher at 7.0 T than at 3.0 T. CNR between cartilage and bone was lower at 7.0 T than at 3.0 T due to an ineffective fat saturation. FIESTA-C images (*middle row*): SNR and CNR values were higher for 7.0 T than for 3.0 T. SPGR images (*lower row*): SNR and CNR values were higher at 7.0 T than at 3.0 T. Diagnostic image quality was not significantly different between both field strengths

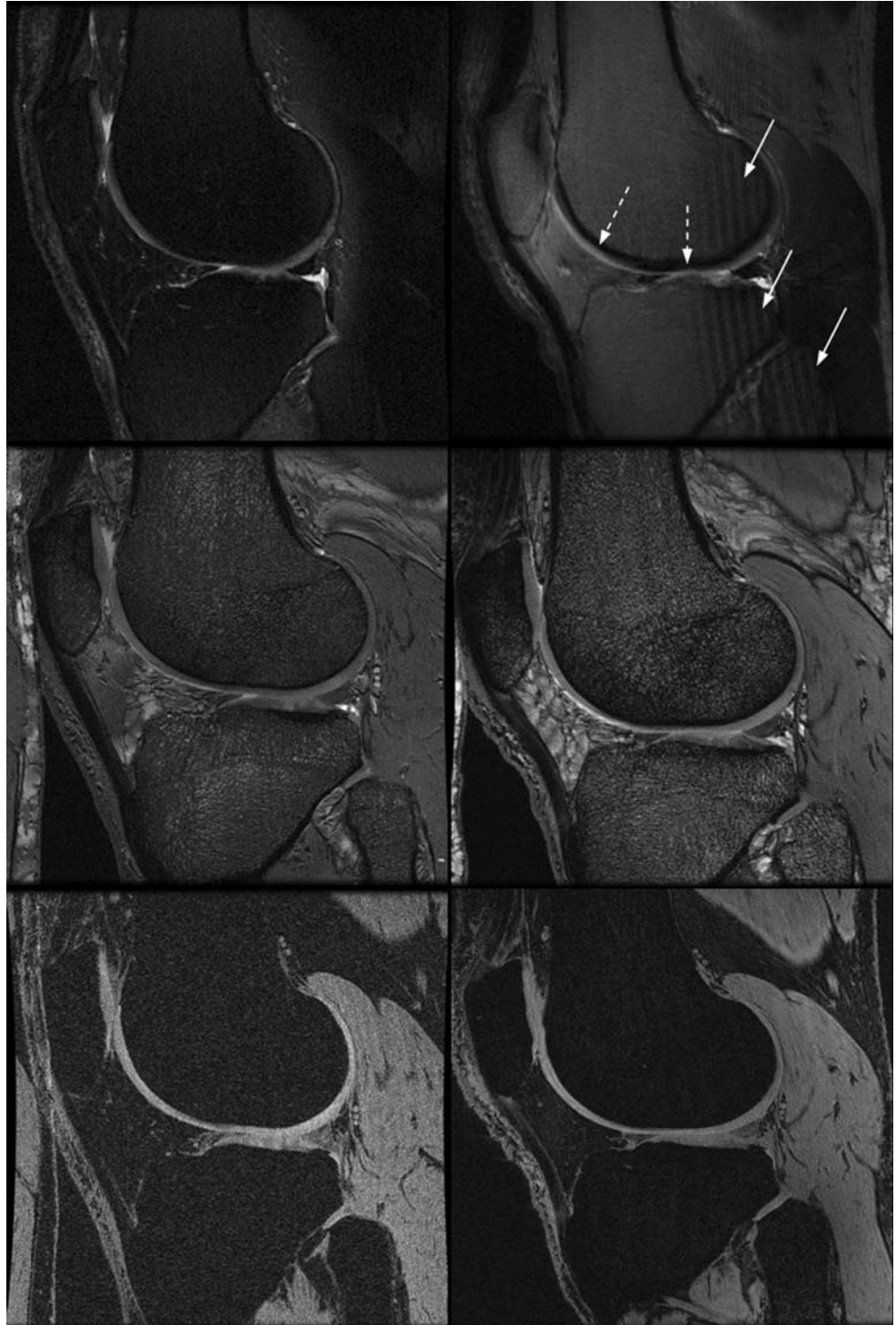
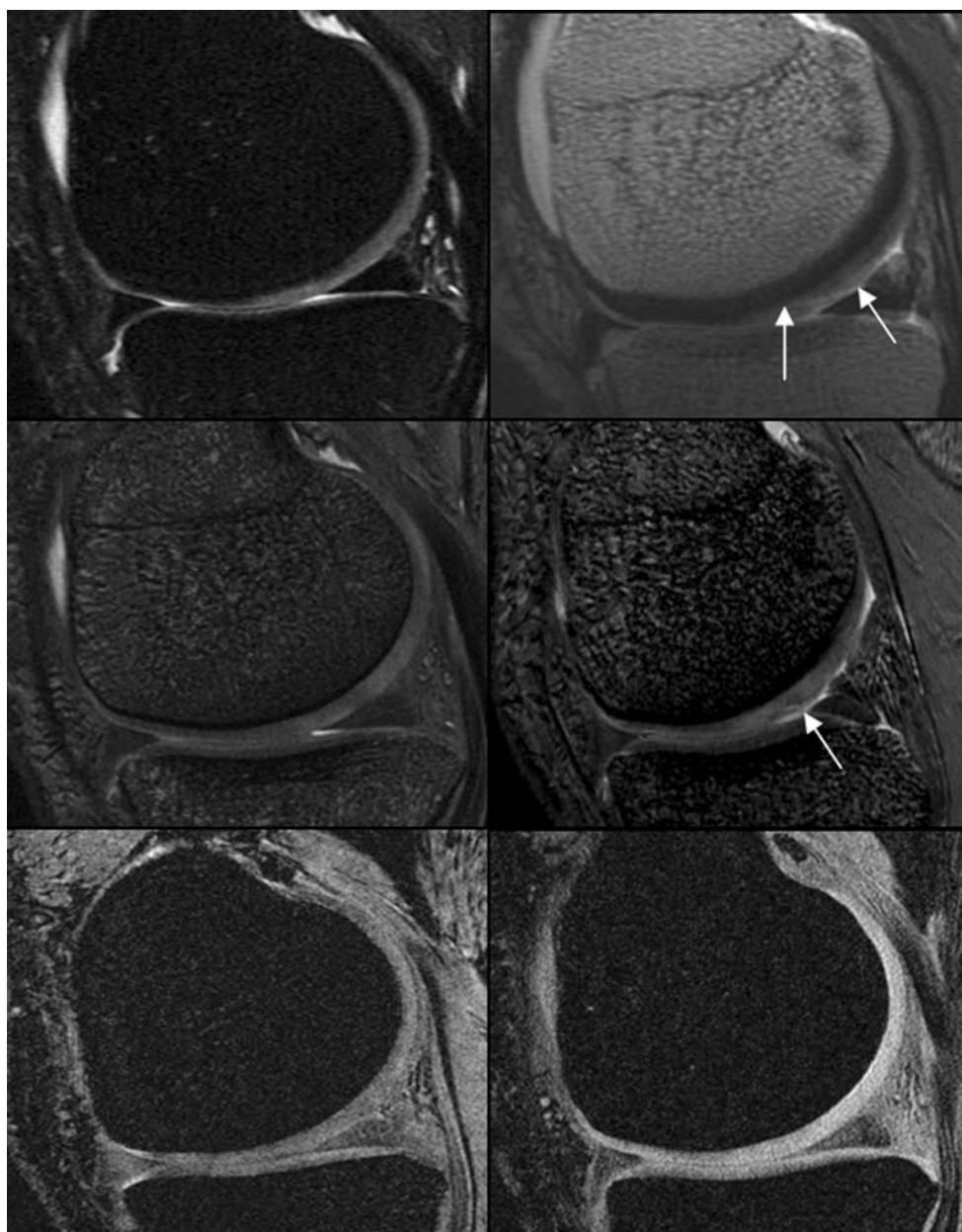


Fig. 2 IM-w (upper row), FIESTA-C (middle row) and SPGR (lower row) images of the medial compartment in a 39-year old healthy male at 3.0 T (left) and 7.0 T (right). IM-w images at 7.0 T show a cartilage fissure (WORMS score 2) at the medial femoral condyle. The maximal extent in sagittal orientation is depicted by the *arrows*. This lesion is also visible at the FIESTA-C images at 7.0 T, but not to its full extent. It was not detected by the radiologists on the SPGR images at 7.0 T as well as on all 3.0 T images. Note the ineffective fat saturation of the IM-w images at 7.0 T



femur, and one at the medial tibia. Three of them were not visualized at 7.0 T (Fig. 3).

Five areas of BMED were congruently detected at both field strengths in three subjects [cumulative WORMS BMED score of these subjects: 2 (1, 2) at 7.0 T; 2 (2, 2) at 3.0 T]. However, in two of these subjects, the size of bone marrow edema at the medial compartment had a score of 2 at 3.0 T and a score of 1 at 7.0 T (Fig. 4).

In two subjects, a small joint effusion (score of 1) was visualized at 7 T, which could not be seen at 3.0 T. In one patient, a joint effusion (score of 1, Fig. 5) and a subchondral cyst (score of 2) at the medial patella was only visible at 3.0 T and not at 7.0 T.

One subject showed a non-displaced tear (score of 2) of the posterior horn of the lateral meniscus at 7.0 T which could not be detected at 3.0 T. However, the distribution and the extent of the findings reported above was not significantly different between the field strengths ($p > 0.05$)

Size of cartilage abnormalities and BMED

Only cartilage lesions which fell in the same category (inhomogeneity or surface defect) at both field strengths were included in the calculation. Size of cartilage inhomogeneities (WORMS=1) was $66.0 \pm 9.1 \text{ mm}^3$ at 3.0 T and $65.0 \pm 8.7 \text{ mm}^3$ at 7.0 T. Size of cartilage lesions (WORMS \geq 2)

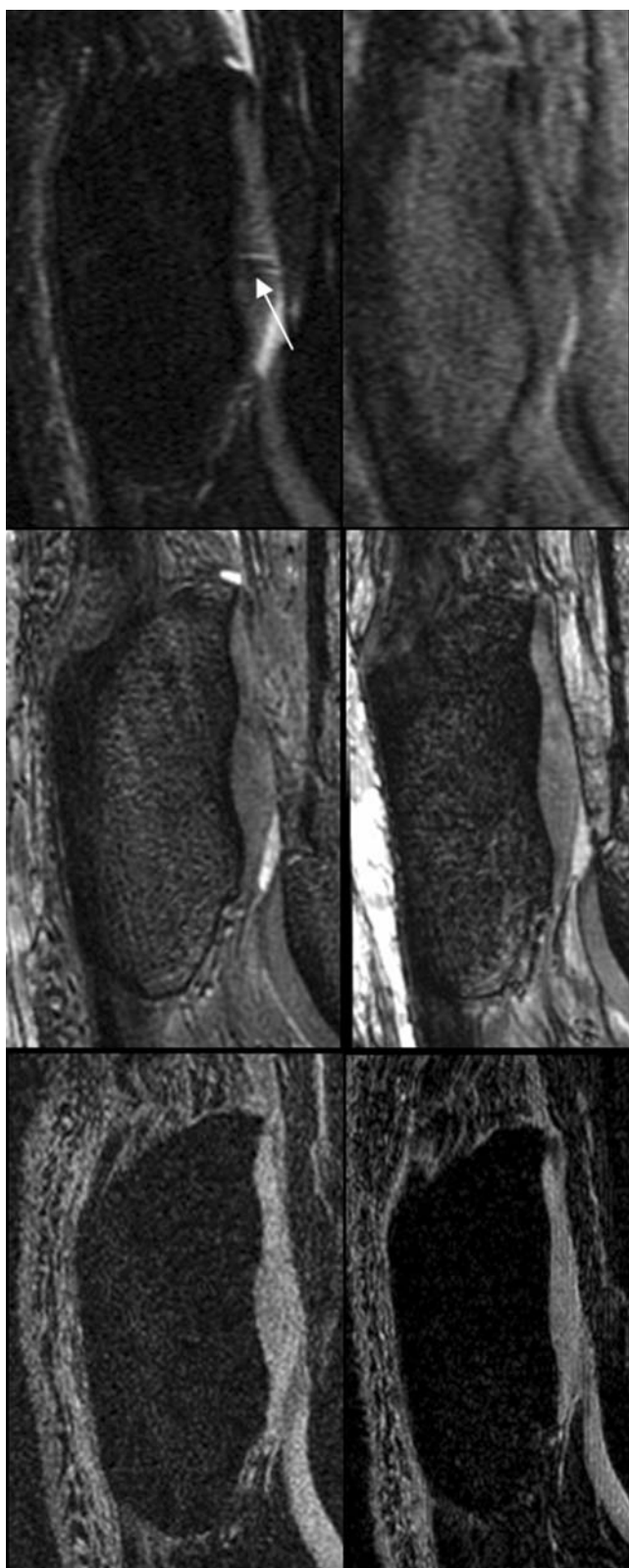


Fig. 3 IM-w (upper row), FIESTA-C (middle row) and SPGR (lower row) images of the lateral patella in a 48-year old male with mild OA obtained at 3.0 T (left) and 7.0 T (right). At 3.0 T, a fissure of the cartilage (grade 2) is clearly depicted at the IM-w images. It was neither detected on the FIESTA-C and SPGR images at 3.0 T nor at all images acquired at 7.0 T. Note the ineffective fat saturation of the IM-w images at 7.0 T

Reproducibility of the quantitative MRI measurements

The root mean square coefficient of variation percentage values (CV%) for the inter-observer, intra-scan setting at 3.0 T were 3.95% for the cartilage signal inhomogeneity, 3.11% for the cartilage lesion size, and 3.43% for the bone marrow edema score. The values at 7.0 T were 3.67%, 3.44%, and 3.98%, respectively.

Sequence confidence rating

The confidence score (CS) of the IM-w sequence for cartilage abnormalities was 53 at 3.0 T and 37.5 at 7.0 T. These values were higher than those for the SPGR (CS=−33 for 3.0 T; CS=−28.5 for 7.0 T) and the FIESTA-C (CS=21 for 3.0 T; CS=24.5 for 7.0 T) sequence. However, regarding the distribution of the underlying confidence levels, these differences between the sequences at both field strengths were not statistically significant ($p>0.324$). Cartilage abnormalities assessed with the FIESTA-C sequence were rated with a significantly higher ($p<0.01$) certainty at 7.0 T than at 3.0 T, particularly at the medial patella (Fig. 6).

Confidence scores in the detection of BMPEP were significantly higher ($p<0.05$) with the IM-w sequence (CS=68.5 for 3.0 T; CS=14 for 7.0 T) compared to the SPGR (CS=−36 for 3.0 T; CS=−34 for 7.0 T) and FIESTA-C (CS=−67.5 for 3.0 T; CS=−67 for 7.0 T) sequence for both field strengths, particularly in the compartments of the medial and lateral femur, the medial and lateral patella, as well as in the lateral tibia. In addition, the IM-w sequence at 3.0 T performed noticeably better ($p<0.001$) at 3.0 T compared to 7.0 T (Fig. 7).

Diagnostic confidence in the assessment of meniscal lesions was significantly different ($p<0.05$) among the studied sequences and among both field strengths (Table 3). The amount of questionable lesions was higher at 7.0 T for the IM-w and SPGR sequence and lower for the FIESTA-C sequence. Absence of loose bodies was diagnosed with a significantly higher ($p<0.05$) certainty at 3.0 T with the IM-w and SPGR sequence than at 7.0 T (Table 3). Integrity of the cruciate ligament structures was diagnosed with a significantly higher ($p<0.05$) confidence with the FIESTA-C sequence at 3.0 T than at 7.0 T (Table 3).

was $69.8\pm 36.9\text{ mm}^3$ at 3.0 T and $65.9\pm 33.7\text{ mm}^3$ at 7.0 T. Mean size of BMPEP was $1,622.0\pm 978.3\text{ mm}^3$ at 3.0 T and $1,138.0\pm 873.4\text{ mm}^3$ at 7.0 T. These findings were not statistically different ($p>0.05$).

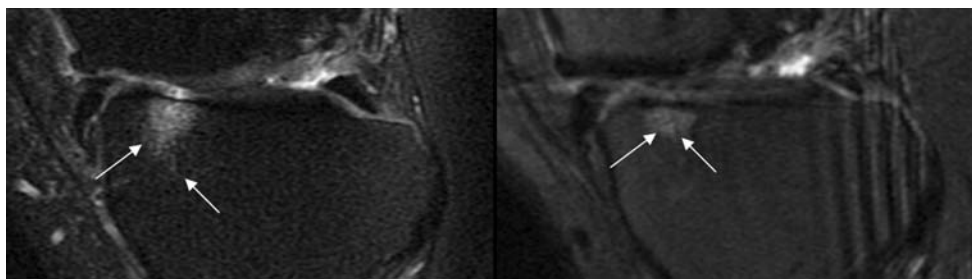


Fig. 4 IM-w images of the medial tibia in a 36-year old male with secondary degenerative changes after osteochondral autograft at 3.0 T (left) and 7.0 T (right). The extent of the BMEP is larger at 3.0 T

(arrows). Consequently, it was rated as a grade 2 lesion at 3.0 T and as a grade 1 lesion at 7.0 T. Note the ineffective fat saturation of the IM-w images at 7.0 T

Image quality

At 3.0 T, the overall image quality score achieved the highest values with the IM-w FSE followed by the FIESTA-C sequence (Table 4, Fig. 3). The SPGR sequence obtained the lowest score. These values were significantly different ($p < 0.05$). At 7.0 T, the overall image quality was significantly ($p < 0.05$) decreased for the IM-w FSE sequence compared to the other sequences (Table 4) due to extensive chemical shift artifacts and pulsation artifacts in the posterior parts of the bones (Fig. 1). Image quality was significantly increased ($p < 0.05$) for the FIESTA-C sequence. Consequently at 7.0 T, FIESTA-C image quality was significantly higher ($p < 0.05$) than the IM-w and SPGR image quality.

Discussion

In this study, we sought to investigate the diagnostic potential of UHF-MRI with regard to degenerative changes of the knee joint. For this purpose, we adapted and optimized three cartilage-dedicated MRI-sequences, which had been previously evaluated at 3.0 T [3], to a 7.0 T scanner and compared qualitative and quantitative findings

between HF- and UHF-technique including SNR, CNR, image quality, diagnostic confidence, and morphological scores characterizing the extent of OA. We also used similar quadrature knee coils for both field strengths in order to compare SNR more accurately.

SPGR and FIESTA-C sequences were applied at UHF-MRI without any difficulty. In comparison to 3.0 T, TE was reduced at 7.0 T for both gradient echo sequences. TR at 7.0 T was slightly elevated for the SPGR sequence in order to compensate for increased T1 at the higher field strength but was slightly reduced for the FIESTA-C sequence in comparison to 3.0 T. For this fully balanced steady-state pulse sequence, the shortest TR possible is desirable as previously discussed [16].

In contrast, when using IM-w FSE sequences, SAR limitations became a major problem. This resulted in interruptions of the scan time with substantial prolongation of the scan time which induced motion artifacts as many patients struggled to keep perfectly still for this period. Therefore, a trade-off between scan time and SAR restrictions had to be made, leading to incomplete coverage of the joint. In addition, extensive chemical shift and pulsation artifacts were observed for that sequence. This is mainly due to inaccurate refocusing pulses.

Fig. 5 IM-w images of a joint effusion at the lateral compartment in a 53 year old male with mild OA at 3.0 T (left) and 7.0 T (right). At 3.0 T, the effusion is clearly visible as a bright area. At 7.0 T, the effusion was missed by the both radiologists. This was caused by multiple interruptions of the scanner due to SAR restrictions. The resulting images looked visually like T1 weighted images where fluid appeared as a dark area (arrows). Note the ineffective fat saturation of the IM-w images at 7.0 T

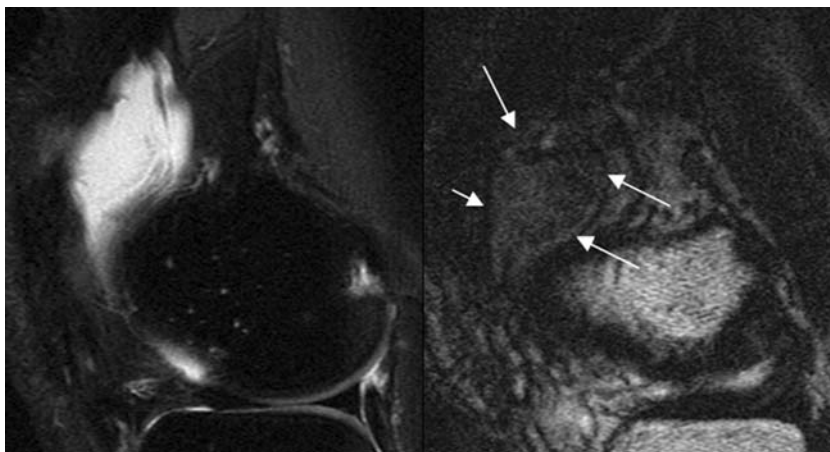
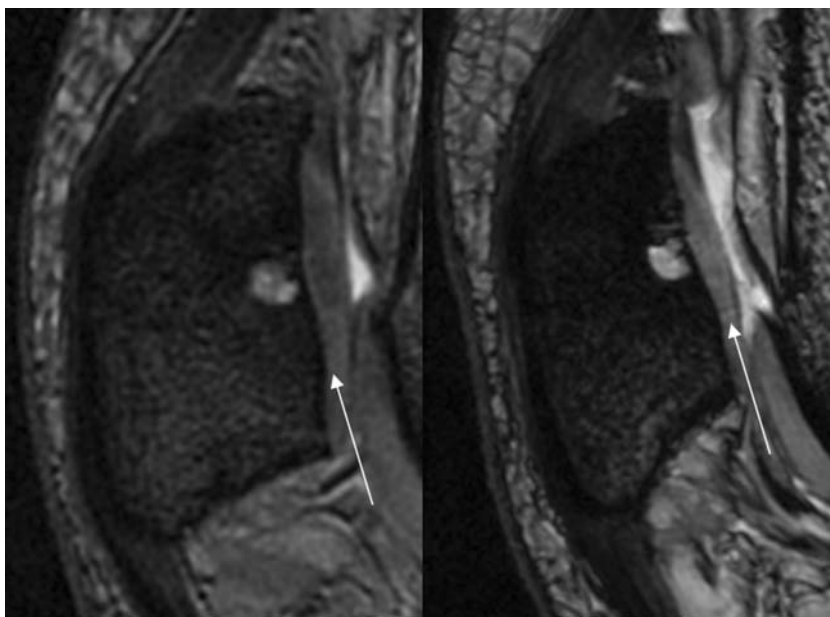


Fig. 6 FIESTA-C images of the medial patella in a 30 year old female with osteoarthritis at 3.0 T (*left*) and 7.0 T (*right*). At 7.0 T a fissure of the cartilage is clearly visible (*arrow*) and a confidence score of 5 (“definitely a lesion”) was assigned. At 3.0 T, a questionable small line can be detected at this location at best (*arrow*), which could have been also caused by an artifact. Consequently, a confidence score of 2 (“most likely no lesion”) was assigned



Although a great effort was made to optimize this sequence, large radio frequency pulses yield a larger amount of energy deposition in the body. This SAR limit cannot be altered without exposing the subject to prohibitive body heating. Potential methods to reduce SAR can be the usage of parallel imaging. This technique generally requires fewer phase encoding steps per image, and the total power deposited in the tissue will be proportionately less at any field strength. At higher field strengths, lower noise amplification factors are generally found [21] allowing higher acceleration and still fewer phase encoding steps without significant image degradation. Multichannel receive coils that have higher intrinsic sensitivity over the volume of interest can reduce the total power deposited in the tissue by reducing the number of signal averages

required to produce images with acceptable signal to noise ratio and by enabling parallel imaging with higher acceleration factors. However, radiofrequency transmit is very challenging with multichannel coils but yet required at UHF-MRI, since on most systems, there is no body transmit installed. In addition, prolonging TR or decreasing the ETL are further options to maintain a lower SAR, but both effect the total scan time.

The increase in SNR of all sequences when moving from 3.0 to 7.0 T followed the basic laws of NMR physics. It was the highest for the FIESTA-C sequence and in concordance with Krug et al. [17]. However, the expected increase in CNR between cartilage and the subchondral bone was not observed for the IM-w FSE sequence at UHF-MRI. This was caused by less effective fat suppression

Fig. 7 IM-w images of the lateral compartment in a 29-year old female with mild OA at 3.0 T (*left*) and 7.0 T (*right*). At 3.0 T, no BMEP could be delineated and a confidence score of 1 (“definitely not a lesion”) was assigned. At 7.0 T extensive pulsation artifacts in the posterior parts of the bones occurred. Consequently, a confidence score of 2 (“most likely no lesion”) was assigned. Note the ineffective fat saturation of the IM-w images at 7.0 T

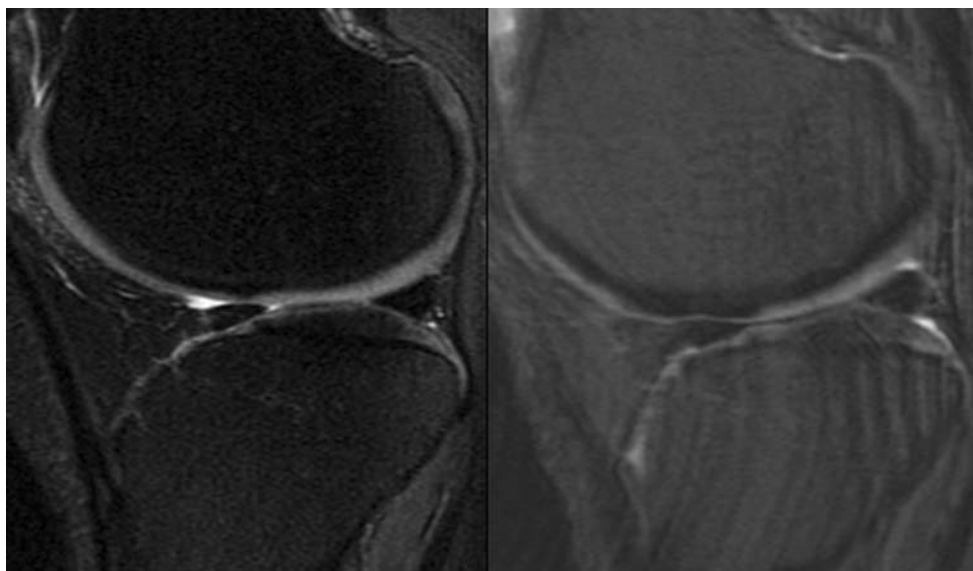


Table 3 Meniscus and other pathology confidence levels for each sequence and both field strengths

Abnormality	Sequence	3.0T	7.0T	<i>p</i> value
Meniscal lesion	IM-w	1 (1, 1)	1 (1, 1.75)	0.005
	SPGR	2 (2, 3)	3 (2, 3)	0.046
	FIESTA	2 (2, 2)	1.5 (1, 2)	0.005
Loose bodies	IM-w	1 (1, 1)	1 (1, 1)	0.046
	SPGR	2 (2, 3)	3 (2, 3)	0.008
	FIESTA	2 (1, 2)	2 (1, 2)	0.655
Anterior/Posterior cruciate ligament	IM-w	1 (1, 1)	1 (1, 1)	0.157
	SPGR	2 (2, 3)	2 (2, 2.75)	0.083
	FIESTA	2 (1, 2)	1 (1, 1.75)	0.007

Results are median values and interquartile ranges (25%, 75%). *p* values in bold indicate significant differences on the 5% level of significance

pulses, leading to brighter signal of the bone marrow on these sequences. In comparison to SPGR, where the fat suppression worked as expected and the same fat suppression method is used, FSE had a different contrast based on T2. Using SPGR, there was less clinically useful contrast between different tissues, and a bright signal highlights the cartilage. The generally larger sensitivity of FSE with respect to SAR limitations and variability of the flip angles might all contribute to a less effective fat suppression. Another potential reason could be found in the decoupling effect of a train of refocusing pulses, increasing the apparent T2 of fatty tissues and render the fat suppression less visible.

Cartilage is the central focus in degenerative joint disease, and early detection of small cartilage lesions is challenging. In our study, we found an equal distribution in the detectability of lesions when comparing both field strengths: some lesions did not change, some were only observed at 3.0 T, and some were only visualized at 7.0 T. However, when assessing the total WORMS scores of areas with cartilage signal inhomogeneities and cartilage surface defects, these values did not differ significantly. Also, when using a more subtle scale by determining the extent of cartilage abnormalities, no significant differences could be observed. BMEP, which is often located in the underlying bone of degenerative cartilage was visualized in a larger area in two subjects when assessed with 3.0 T. This was also true for a small joint effusion and a subchondral cyst, which are both fluid-containing pathologies. Since those

were diagnosed mainly on IM-w FSE sequences, we concluded that this was mostly due to the less effective fat suppression at 7.0 T. However, in our study population, the median compartment-specific WORMS scores and the mean extent of BMEP were not significantly different between the two field strengths. Consequently, the WORMS surface scores and total WORMS scores did not differ between HF- and UHF-MRI.

In comparison to the SPGR and FIESTA-C sequence, the diagnostic confidence scores of the IM-w FSE sequence for evaluating cartilage and BMEP were superior within both field strengths. First, it yields an intermediate cartilage signal with higher intrinsic cartilage contrast and is therefore more sensitive to cartilage internal pathology [22] which has been shown for 3.0 T in a previous study [3]. Second, since at 3.0 T the fat saturation performed better and less artifacts occurred, this sequence had a significantly higher amount of “definitely no BMEP lesions” ratings in comparison to 7.0 T. Accordingly, absence of meniscal lesions and loose bodies were diagnosed with a higher confidence at 3.0 T, since these pathologies are indirectly diagnosed by the shape of the surrounding fluid. We observed only one case of a meniscal tear which could be shown only on the 7.0-T IM-w FSE images.

Consequently, image quality was rated highest for the IM-w FSE sequence at 3.0 T and lowest at 7.0 T. An increase in image quality was observed for the FIESTA-C and SPGR sequence when conducted at 7.0 T. We conclude that this is caused by a simultaneous increase of SNR and CNR in these sequences at UHF, which results in a better delineation of the cartilage borders. In addition, the FIESTA-C sequence has a high cartilage-to-fluid contrast and cartilage lesions appear as filling defects at the cartilage surface. Together with the increased SNR and CNR, we believe this is the cause for yielding a higher amount of “definitely a lesion”-ratings when conducted at 7.0 T. According to previously published results [3, 7], the SPGR sequence had the lowest confidence levels for diagnosing cartilage lesions and BMEP at both field strengths. The

Table 4 Sequence and field strength comparison: overall image quality score (mean±standard deviation)

Sequence	3.0T	7.0T	<i>p</i> Value
IM-w	3.80±0.42	2.60±0.97	0.005
SPGR	2.30±0.68	2.70±0.48	0.168
FIESTA-C	3.20±0.63	3.80±0.63	0.024

p values in bold indicate significant differences on the 5% level of significance

bright appearance of the cartilage signal, which well demarcates the bone–cartilage interface and—to a remarkably lower extent—the synovial fluid, makes this sequence more suitable for segmentation algorithms to determine cartilage volume and thickness [23].

A limitation of this study is the low number of subjects. In addition, subjects did not undergo arthroscopy, which could be used as a reference to validate our MRI findings. However, we focused on differences of the MRI morphology when assessed with both field strengths. This was the reason why the examinations on both scanners were performed within a short period. Also, diagnostic performance in detecting cartilage abnormalities has been validated in previous studies [24, 25].

In conclusion, this study indicates that IM-w FSE sequences may be less feasible at 7.0 T than at 3.0 T for assessment of OA-induced-changes. At 7.0 T, a dramatic decrease of the performance parameters of IM-w FSE sequences was found: more artifacts, lower image quality, and lower diagnostic confidence, less effective fat saturation, and SAR limitations, which makes this sequence not yet feasible for clinical application. This is in agreement with Kraff et al. [12] who observed similar results with a turbo spin echo sequence. In contrast, SPGR and FIESTA-C sequences are well suited for imaging at 7.0 T yielding higher SNR and CNR. This may be used to enhance image spatial resolution. For SPGR sequences, this may improve the analysis of cartilage volume when assessed with manual or automatic segmentation techniques. For FIESTA-C sequences, this may also improve early detection of cartilage lesions.

Acknowledgements We would like to thank Niles Bruce from the Musculoskeletal and Quantitative Imaging Research Group at the University of California, San Francisco, San Francisco, CA, USA for their help with the subject scans.

Open Access This article is distributed under the terms of the Creative Commons Attribution Noncommercial License which permits any noncommercial use, distribution, and reproduction in any medium, provided the original author(s) and source are credited.

References

- Link TM, Sell CA, Masi JN, Phan C, Newitt D, Lu Y, et al. 3.0 vs 1.5 T MRI in the detection of focal cartilage pathology—ROC analysis in an experimental model. *Osteoarthritis Cartilage* 2006;14(1): 63–70.
- Kornaat PR, Reeder SB, Koo S, Brittain JH, Yu H, Andriacchi TP, et al. MR imaging of articular cartilage at 1.5 T and 3.0 T: comparison of SPGR and SSFP sequences. *Osteoarthritis Cartilage* 2005;13(4): 338–344.
- Stahl R, Luke A, Ma CB, Krug R, Steinbach L, Majumdar S, et al. Prevalence of pathologic findings in asymptomatic knees of marathon runners before and after a competition in a comparison with physically active subjects—a 3.0 T magnetic resonance imaging study. *Skeletal Radiol* 2008;37(7): 627–638.
- Barr C, Bauer JS, Malfair D, Ma B, Henning TD, Steinbach L, et al. MR imaging of the ankle at 3 Tesla and 1.5 Tesla: protocol optimization and application to cartilage, ligament and tendon pathology in cadaver specimens. *Eur Radiol* 2006;17: 1518–1528.
- Fischbach F, Bruhn H, Unterhauser F, Ricke J, Wieners G, Felix R, et al. Magnetic resonance imaging of hyaline cartilage defects at 1.5 T and 3.0 T: comparison of medium T2-weighted fast spin echo, T1-weighted two-dimensional and three-dimensional gradient echo pulse sequences. *Acta Radiol* 2005;46(1): 67–73.
- Kuo R, Panchal M, Tanenbaum L, Crues JV 3rd. 3.0 Tesla imaging of the musculoskeletal system. *J Magn Reson Imaging* 2007;25(2): 245–261.
- Masi JN, Sell CA, Phan C, Han E, Newitt D, Steinbach L, et al. Cartilage MR imaging at 3.0 versus that at 1.5 T: preliminary results in a porcine model. *Radiology* 2005;236(1): 140–150.
- Saupe N, Prussmann KP, Luechinger R, Bosiger P, Marincek B, Weishaupt D. MR imaging of the wrist: comparison between 1.5- and 3-T MR imaging—preliminary experience. *Radiology* 2005;234(1): 256–264.
- Griffin N, Joubert I, Lomas DJ, Bearcroft PW, Dixon AK. High resolution imaging of the knee on 3-Tesla MRI: a pictorial review. *Clin Anat* 2008;21(5): 374–382.
- Pakin SK, Cavalcanti C, La Rocca R, Schweitzer ME, Regatte RR. Ultra-high-field MRI of knee joint at 7.0 T: preliminary experience. *Acad Radiol* 2006;13(9): 1135–1142.
- Regatte RR, Schweitzer ME. Ultra-high-field MRI of the musculoskeletal system at 7.0 T. *J Magn Reson Imaging* 2007;25(2): 262–269.
- Kraff O, Theysohn JM, Maderwald S, Saylor C, Ladd SC, Ladd ME, et al. MRI of the knee at 7.0 Tesla. *Rofo* 2007;179(12): 1231–1235.
- Peterfy CG, Guermazi A, Zaim S, Tirman PF, Miaux Y, White D, et al. Whole-Organ Magnetic Resonance Imaging Score (WORMS) of the knee in osteoarthritis. *Osteoarthritis Cartilage* 2004;12(3): 177–190.
- Kellgren JH, Lawrence JS. Radiological assessment of osteoarthritis. *Ann Rheum Dis* 1957;16(4): 494–502.
- Haacke EM, Wielopolski PA, Tkach JA, Modic MT. Steady-state free precession imaging in the presence of motion: application for improved visualization of the cerebrospinal fluid. *Radiology* 1990;175(2): 545–552.
- Banerjee S, Han ET, Krug R, Newitt DC, Majumdar S. Application of refocused steady-state free-precession methods at 1.5 and 3 T to in vivo high-resolution MRI of trabecular bone: simulations and experiments. *J Magn Reson Imaging* 2005;21(6): 818–825.
- Krug R, Carballido-Gamio J, Banerjee S, Stahl R, Carvajal L, Xu D, et al. In vivo bone and cartilage MRI using fully-balanced steady-state free-precession at 7 Tesla. *Magn Reson Med* 2007;58(6):1294–8.
- Krug R, Han ET, Banerjee S, Majumdar S. Fully balanced steady-state 3D-spin-echo (bSSSE) imaging at 3 Tesla. *Magn Reson Med* 2006;56(5): 1033–1040.
- Barr C, Bauer JS, Malfair D, Ma B, Henning TD, Steinbach L, et al. MR imaging of the ankle at 3 Tesla and 1.5 Tesla: protocol optimization and application to cartilage, ligament and tendon pathology in cadaver specimens. *Eur Radiol* 2007;17(6): 1518–1528.
- Gluer CC, Blake G, Lu Y, Blunt BA, Jergas M, Genant HK. Accurate assessment of precision errors: how to measure the

- reproducibility of bone densitometry techniques. *Osteoporos Int* 1995;5(4): 262–270.
21. Wiesinger F, Van de Moortele PF, Adriany G, De Zanche N, Ugurbil K, Pruessmann KP. Parallel imaging performance as a function of field strength—an experimental investigation using electrodynamic scaling. *Magn Reson Med* 2004;52(5): 953–964.
 22. Link TM, Stahl R, Woertler K. Cartilage imaging: motivation, techniques, current and future significance. *Eur Radiol* 2006;17: 1135–1146.
 23. Potter HG, Foo LF. Magnetic resonance imaging of articular cartilage: trauma, degeneration, and repair. *Am J Sports Med* 2006;34(4): 661–677.
 24. Figueroa D, Calvo R, Vaisman A, Carrasco MA, Moraga C, Delgado I. Knee chondral lesions: incidence and correlation between arthroscopic and magnetic resonance findings. *Arthroscopy* 2007;23(3): 312–315.
 25. Friemert B, Oberlander Y, Schwarz W, Haberle HJ, Bahren W, Gemgross H, et al. Diagnosis of chondral lesions of the knee joint: can MRI replace arthroscopy? A prospective study. *Knee Surg Sports Traumatol Arthrosc* 2004;12(1): 58–64.